Mountain Risks: 2007-2010
A Marie Curie Research & Training Network
http://mountain-risks.eu

Multi-date correlation of Terrestrial Laser Scanning data for the characterization of landslide kinematics

J. Travelletti (1,2), J.-P. Malet (1), C. Delacourt (3)

(1) Institut de Physique du Globe de Strasbourg, CNRS UMR 7516, University of Strasbourg (EOST), 5 rue René Descartes, 67084 Strasbourg Cedex, France
(2) GEOPHEN-LETG, CNRS UMR 6554, University of Caen Basse-Normandie, 14032 Caen Cedex, France
(3) Université Européenne de Bretagne, Institut Universitaire de la Mer, CNRS UMR 6538, University of Brest, Brest, France

Contact: Julien Travelletti
Institut de Physique du Globe de Strasbourg, CNRS UMR 7516, University of Strasbourg (EOST), 5 rue René Descartes, 67084 Strasbourg Cedex, France
Email: julien.travelletti@unistra.fr

EGU2011-10302-1

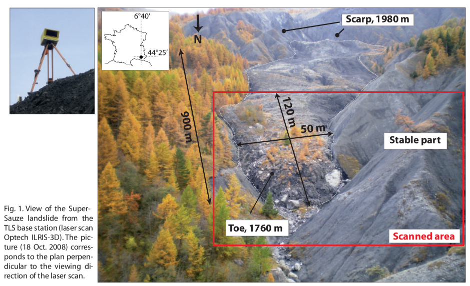

Fig. 1. View of the Super-Sauze landslide from the TLS base station (laser scan Optech ILRIS-3D). The picture (18 Oct. 2008) corresponds to the plan perpendicular to the viewing direction of the laser scan.

Objective

This work presents a simple method to characterize the 3D displacement field of landslide by exploiting all geometrical information contained in 3D point clouds with a normalized cross correlation function. The toe of the Super-Sauze landslide (South French Alps) is chosen as an experimental site (Fig. 1). The landslide extents over a distance of 900 m between an elevation of 1980 m at the crown and 1760 m at the toe with an average width of 135 m and a average slope of 25° (Malet et al., 2002).

Acquisition of TLS data

The monitoring has been realized with a long-range terrestrial laser scan Optech ILRIS-3D (Fig. 1). Ten acquisitions were acquired between October 2007 and May 2010 for the same base station at an average distance of 100 m from the landslide. The point clouds are constituted of 9 to 12 millions of points distributed on a surface of 6'000 m² (average point density of 230 pt.m²)

Co-registration and georeferencing

Each TLS dataset is aligned with a 3D error of ±4 cm on the stable parts surrounding the landslide. For the georeferencing, an Airborne Laser Scanning (ALS) point cloud was used as a reference (Fig. 2). The georeferencing accuracy presents an average error of ±1 cm and a standard deviation of 14 cm.

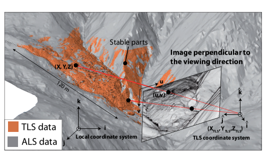

Fig. 2. Alignment of the stable parts of the different TLS point clouds on the ALS point cloud, with indication on the projective projection applied on the TLS point clouds with the different coordinate systems involved in the procedure.

Simplification of the 3D matching problem

A projective transformation allows to represent the entire geometrical information in a plan perpendicular to the viewing direction of the scan. The relationship among the 3D position (X,Y,Z) of each point in the ground reference system to its position (u,v) in the plane reference system is given by the collinearity equations (Kraus and Waldhaüsel, 1994) (Fig. 2). A scaling factor is used to adjust the average point density to 1 pt.pixel^{-1} to preserve the geometrical information. The 2D gradient of the distance between the point clouds and the TLS station is calculated for emphasizing the morphology of the landslide. The generated images are then converted in grey-scale values (Fig. 3).

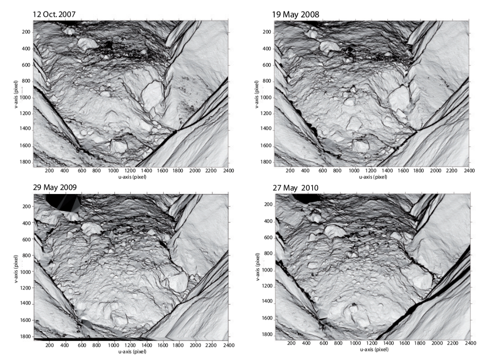

Fig. 3. Images derived from the gradient calculation on the TLS point clouds at different dates.

Determination of the displacement field by image correlation

The image correlation principle consists in recognizing identical intensity distribution patterns in a correlation window over two images to determine the displacement of the center of the window by maximizing a normalized cross correlation function (Lewis, 1995).

The result of the correlation corresponds to the displacements Δu and Δv along the u-axis and v-axis. To reconstruct the 3D displacement field, a triplet of coordinates (X,Y,Z) obtained from the first and the second TLS acquisitions is associated to each initial (u,v) and final position $(u+\Delta u, v+\Delta v)$ of the displacement vectors in the images. The median of the displacement components $(\Delta X, \Delta Y, \Delta Z)$ located in the same mesh (one-meter grid mesh size) is then computed.

Strain computation

A strain analysis is applied to characterize possible different behaviours in the landslide material. A local least square fitting technique is used to compute the Cauchy's strain tensor **E** at each location of the grid (Pan et al., 2009). The two eigenvalues e_1 and e_2 of **E** corresponding to the change of length per unit of length in the direction having the maximum and minimum extension (positive for extension) without shearing are computed. The deformation is presented by the surface strain defined as $\varepsilon_s = e_1 + e_2$ (positive for extension) and the shear strain defined as $\gamma = |e_1 - e_2|$.

Kinematic analysis

For the period July-October 2008, displacements between 0.5 and 1.5 m are observed (average displacement rate of 0.6-1.7 cm.day^{-1}). The largest displacements are detected at the front of the toe (Fig. 4A). For the period July-October 2009, shorter displacements ranging from 0.1 m at the front of the landslide toe to 0.6 m in the upper part of the toe are observed (average displacement rate of 0.1-0.8 cm.day^{-1}; Fig. 4B).

In 2008 and 2009, the upper part of the toe is characterized by a succession of approximately parallel bands (width of 5 to 10 m) in compression and extension which main orientation is perpendicular to the sliding direction (Fig. 4C, D). The behavior at the front of the toe is very different for the two years. In 2008, the extension behavior creates tensile fissures and important shearing located along the landslide boundary (Fig. 4E). This confirmed by the presence of very persistent tensile and shear fissures observed in the field from veru-high resolution images (Fig. 5). In 2009, the deformation affecting the front toe is less important (Fig. 4F).

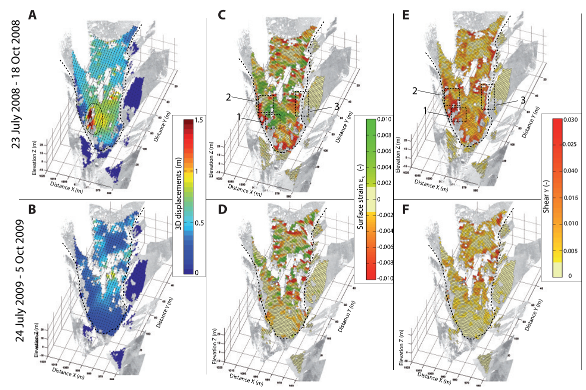

Fig. 4. Results of the displacement and strain calculations for the periods July-October 2008 and July-October 2009. A), B) Calculated 3D displacement field. The shallow slope failure is marked with a dashed line; C), D) Calculated surface strain (positive for extension, negative for compression); E), F) Calculated shear strain. The locations 1, 2 and 3 in C) and E) are related to Fig. 5.

Validation of the computed displacements

The computed displacements are in very good aggreement with the displacements calculated with the Iterative Closest Point algorithm (Besl and McKay, 1992; average error of 2 cm and standard deviation of 2 cm; Fig. 6B) and observed from the GPS monitoring of five blocks at the landslide toe (average error of 4 cm and standard deviation of 3 cm; Fig. 6A, C).

Fig. 6. Comparison of the displacements obtained by correlation with the ICP method and the dGPS monitoring. A) Locations of the blocks in the point cloud; B) Comparison with the ICP method; C) Comparison with the dGPS monitoring.

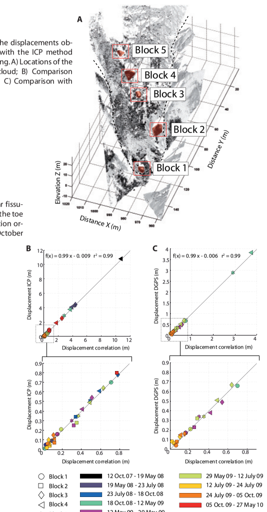

Fig. 5. Tensile fissures (1) and shear fissures (2, 3) observed at the front of the toe (Fig. 4C, E) on a very-high resolution orthophotograph acquired in October 2008 (Niethammer et al., 2010).

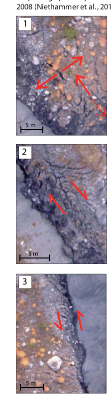

References:
Besl, P., McKay, N, 1992. A method for registration of 3-D shapes. IEEE Trans Pattern Anal Mach Intell, 14, 239-256.
Kraus, K., Waldhäusl, P., 1994. Photogrammetry, Fundamentals and Standard processes. vol 1. Hermès (Eds.), Paris.
Lewis, J.P. 1995. Fast normalized cross-correlation. Vision Interface, 120-123.
Niethammer, U., Rothmund, S., James, M. R., Travelletti, J., Joswig, M. 2010. UAV-based remote Sensing of landslides. International Archives of Photogrammetry, Remote Sensing and Spatial Information Sciences, Vol. XXXVIII, Part 5 Commission V Symposium, Newcastle upon Tyne, UK.
Malet, J.-P., Maquaire, O., Calais, E., 2002. The use of global positioning system techniques for the continuous monitoring of landslides. Geomorphology, 43, 33-54.
Pan, B., Asundi, A., Xie, H., Gao, J. 2009. Digital image correlation using iterative least squares and pointwise least squares for displacement field and strain field measurements. Optics and Lasers in Engineering, 47, 865-874.

MARIE CURIE ACTIONS